doi: 10.82124/CEAS-GNC-2026-062

Tractor-Beam: An Experimental Testbed for Control of In-Orbit Servicing Systems with Varying Flexible Dynamics and Inertia

Jose F. Briz GNC Engineer, GMV Innovating Solutions, Madrid, Spain, *jbriz@gmv.com*

Eduardo de Brito Software Engineer, GMV Innovating Solutions, Lisbon, Portugal, *ebrito@gmv.com*

Instituto Superior Técnico (IST), Lisbon, Portugal

Marco Rubaga Systems Engineer, GMV Innovating Solutions, Lisbon, Portugal, *mrubaga@gmv.com*

Delft University of Technology, Delft, The Netherlands

Mariana Ferreira Structural Engineer, GMV Innovating Solutions, Lisbon, Portugal, *mroldao@gmv.com*

Instituto Superior Técnico, Lisbon, Portugal

Luís Ferreira GNC Engineer, GMV Innovating Solutions, Lisbon, Portugal, *lmferreira@gmv.com*

Instituto Superior Técnico, Lisbon, Portugal

Hugo Pereira GNC Engineer, GMV Innovating Solutions, Lisbon, Portugal, *hpereira@gmv.com*

Diogo Oliveira Software Engineer, GMV Innovating Solutions, Lisbon, Portugal, *doliveira@gmv.com*

Iñaki Colmenarejo Hardware Technician, GMV Innovating Solutions, Madrid, Spain, *icolmenarejo@gmv.com*

Nuno Paulino Project Manager, GMV Innovating Solutions, Lisbon, Portugal, *nuno.paulino@gmv.com*

Pedro Lourenço Section Head Advanced Guidance & Control, GMV Innovating Solutions, Lisbon, Portugal, *palourenco@gmv.com*

Valentin Preda Technical Officer, ESTEC, Noordwijk, The Netherlands, *valentin.preda@esa.int*

ABSTRACT

In the last few years, In-Orbit Servicing, Assembly and Manufacturing (ISAM) has become one of the main and most discussed topics in space operations, ensuring increased flexibility, scalability and allowing mission concepts not feasible with current approaches based on ground assembly. From the point of view of Guidance, Navigation and Control (GNC), one of the main challenges of ISAM operations is accurate control of systems whose properties change over time or are not known precisely, due to recurring operations of docking, separation, assembly and disassembly. Here, we introduce the TRACTOR-beam experimental test rig, used in rapid prototyping and testing for research in control and system identification with time-varying bending modes, inertia properties or additional effects which can be added in a modular fashion. The setup is comprised of a 1 Degree of Freedom (DoF) rotating platform on a low friction support, actuated with a

reaction wheel, and it combines a central hub, a flexible appendage, and a robotic walker that moves along the appendage. The latter allows for variation of inertia and bending properties during the experiments. The setup realizes a ground surrogate experiment which captures the problems and challenges faced during ISAM, with low friction attitude dynamics, the robotic walker changing the system properties by moving on top of the flexible beam, and a space-representative set of sensors and actuators. The TRACTOR platform follows a modular architecture which supports distributed intelligence and modular expansion. A digital twin of the test setup was developed in MATLAB/Simulink, replicating the main dynamic effects, sensors and actuators. The wireless communication interfaces with MATLAB/Simulink provide a streamlined deployment of OBSW and management of the experiment, and an end-to-end validation chain enabling rapid prototyping and testing cycle. The paper provides a description of the test setup, digital twin with its SW interface, and experimental preliminary results in closed-loop, as well as system identification for different mass configurations.

Keywords: ISAM, In-Orbit Assembly, AOCS, Surrogate Experiments, Flexible Structures, Attitude Control, Hardware-in-the-loop, HIL (Hardware-in-the-loop), Validation

Nomenclature

x, θ	=	Position, angle
F_A^B, T_A^B	=	Force, torque of source "B" applied on point "A"
$\mathbf{L}_P$	=	Flexible participation factor matrix in point "P"
$\mathbf{K}, \mathbf{D}$	=	Stiffness and damping matrices for 2nd order systems
$\mathbf{D}_A^B$	=	Generalized mass/inertia matrix of object "B" expressed in point A
σ	=	Friction coefficient
η	=	Modal coordinate
τ_{PG}	=	Matrix to transport linear and accelerations from point G to point P
s	=	Laplace variable
M(s)	=	Generalized transfer function from input torque to output angular acceleration

1 Introduction and Objectives

Within the context of the IOANT project (Guidance, Navigation And Control Of In-Orbit Assembly Of Large Antennas) [1] GMV has defined a series of surrogate experiments, and designed and built a test rig with 1DoF in rotational motion, internal travelling masses with 1DoF in translational motion, and instrumentation for attitude control in the presence of flexible appendages.

The objective of the TRACTOR-Beam (Test Rig for Analysis and Control of Travelling Oscillations in a Resonant Beam) is to provide a scaled proof-of-concept (PoC) to emulate the variation of properties that take place during the assembly of an antenna and study guidance, navigation and control strategies for such applications. It focuses particularly on the attitude dynamics of the spacecraft during the assembly process, subject to disturbances introduced by the elements in charge of the assembly while the properties themselves change over time and the following aspects:

- Time-varying Inertia and Flexible Dynamics: The platform allows the variation of flexible and Mass, Centroiding and Inertia (MCI) properties that take place during the assembly process. The mass moving along the flexible beam changes the physical properties of the system. This mimics the process that happens in-orbit.

- Representative Sensing and Actuation System: The setup uses representative hardware-in-the-loop to replicate the impact that Navigation and Control have on the closed-loop dynamics. The hardware encompasses an attitude encoder and gyroscope to mimic a gyro-stellar suite for Navigation, and a reaction wheel as actuation system to provide torque.
- Modular Design: The rig can be easily upgraded to include additional effects, such as sloshing. Different beams can be easily swapped to test multiple flexible properties, and the system baseline inertia can also be altered.
- Fast Prototyping and Validation: The physics of the system and software architecture are duplicated in MATLAB/Simulink, effectively constituting a digital twin. The platform processor is connected to the Simulink setup wirelessly, and new On-Board Software versions can be uploaded quickly. The combination of these elements provides a very agile way of developing and testing GNC algorithms.
- Increase TRL (Technology Readiness Level): The rig provides a testbench to validate GNC algorithms with PIL (Processor-in-the-loop) and HIL (Hardware-in-the-loop) tests, increasing the TRL of the SW and corresponding algorithms.

There is a wide variety of available test rigs with representative dynamics for space applications. One setup whose concept is very similar to TRACTOR-Beam is the BAMOSS [2] where flexible dynamics were excited through a pair of flexible appendages attached to a central hub at one end and carrying discrete masses at their free ends. The main novelty of TRACTOR resides in the possibility of changing the position of the mass, also referred to as the robotic walker, changing the system properties during experiments. It also features a modular approach, which facilitates quick modifications and the addition of elements to test different dynamics. Similarly, the integration with MATLAB/Simulink allows the deployment of new controllers in just a few minutes, providing rapid prototyping capabilities.

Other families of testing platforms which could be compared with the objectives of TRACTOR-Beam include:

- Platforms with 3DOF: They are usually air bearing platforms levitating a few millimetres on a flat surface, allowing for 2 translational DOF and 1 rotational DOF. They need to be carefully balanced to avoid lateral rotations, which can produce an imbalance that causes contact with the ground and introduces undesired torques, limiting the range of MCI changes that can be introduced. The experiments are also limited in time by the availability of gas to maintain levitation and provide translation control. Some examples of these platforms are KNATTE by LTU Sweden [3], PINOCCHIO by Sapienza University [3], SOOST by NUAA [4], or SRE by NTUA [5].
- Platforms with 6DOF: They are usually composed of one or more robotic manipulators that can change the relative position and attitude of the experimental elements, emulating the system dynamics. However, these usually require a parallel simulator in the loop to propagate a dynamic model, since the manipulators used are restricted kinematically. Some examples of these platforms are platform-art© by GMV [6], ESA's GRALS [7], the HIL testbed by Shenzhen Space Technology Center [8], European Proximity Operations Simulator by DLR [9] or SPDM verification facility by the Canadian Space Agency [10]. These platforms provide high-fidelity navigation inputs but for the purpose of controlling a dynamic system, they are not fully representative.

The rig in Fig. 1 depicts the TRACTOR-Beam platform and its primary elements.

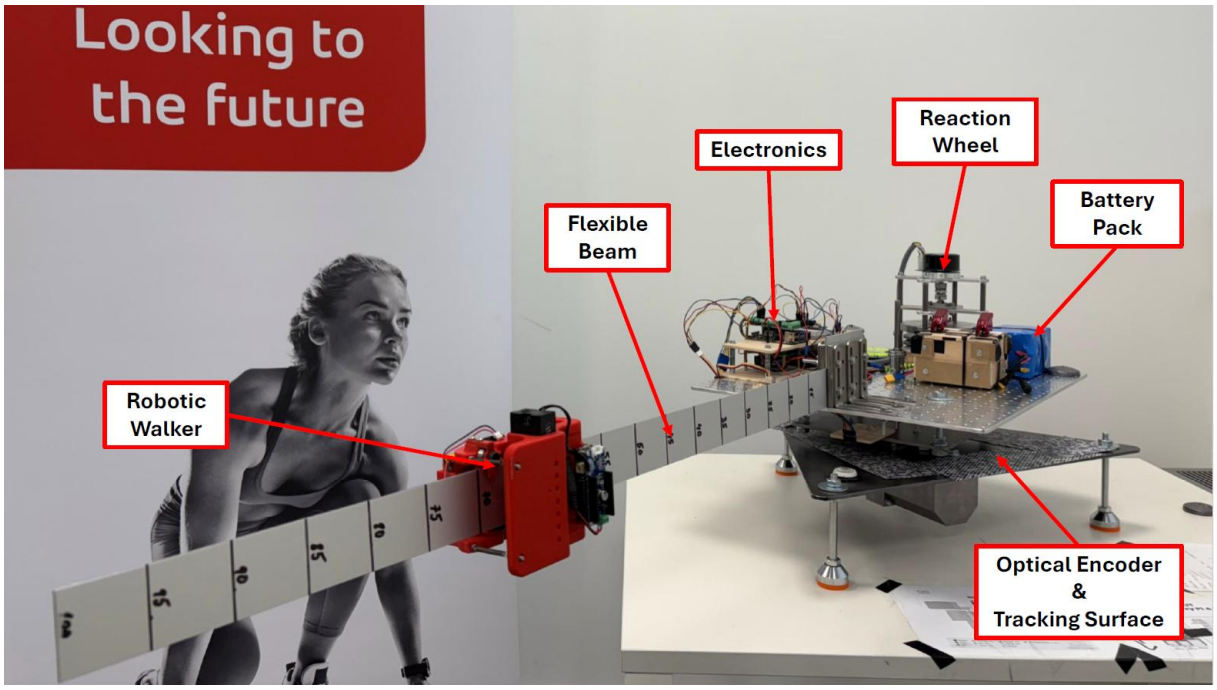

Fig. 1: TRACTOR-beam platform featuring a moving walker for time-varying MCI and bending properties.

2 Experimental Platform Description

The platform design covers the main experimental objectives, primarily the variation of properties and space representativeness, while accounting for robustness and safety. The design decisions address the variation of flexible and MCI properties, as well as the representativeness of the space dynamics and hardware.

A more detailed description of how the system parameters affect the flexible properties is provided in Sections 2.2 and 3.1. The key point is that the characteristics of the beam, along with the walker mass and position, determine the natural frequencies of the system. To maximize the testing envelope of frequencies, it is necessary a fine trade-off between range of frequencies and achievable MCI properties:

- Longer, more flexible beams offer a broader range of motion for the sliding mass, and consequently larger variations in frequency and inertia. However, longer beams are more prone to structural instabilities (torsion), and the centre-of-mass offset can increase the strain on the platform rotation system, increasing the friction or even the risk of breaking the structure.
- Beams with higher flexibility yield lower resonant frequencies but there is a practical limitation in very low frequencies, since the duration of the experiments would have to be extended to observe multiple oscillations of the beam. Additionally, if the system is too flexible, static structural instabilities can appear and potentially break the setup.
- Stiffer beams yield higher resonant frequencies, and exceedingly high resonant frequencies cannot be actively controlled, either because the required control authority is too high, the actuation system demands an exceptionally high bandwidth, or the navigation and GNC cannot observe them properly. This means that there is also a practical limitation of the high end of the frequency envelope.

With regards to space representativeness, there are a series of effects that need to be accounted for. A more detailed description is also provided and justified in Sections 2.1 and 2.4. The friction needs to

be minimized to reduce the strain on the control system and not affect the flexible dynamics. This is achieved in the platform minimizes the number of contact points on their surfaces to reduce friction. The setup is completely wireless to reduce hanging elements with the data transfer performed via wi-fi, and system electronics powered by a battery. The sensors and actuators are similar in nature to those used in space applications, including a reaction wheel and sensors that emulate space star trackers and gyroscopes.

Fig. 2 illustrates the concept for the platform based on the considerations listed above. The following subsections describe the platform elements in more detail.

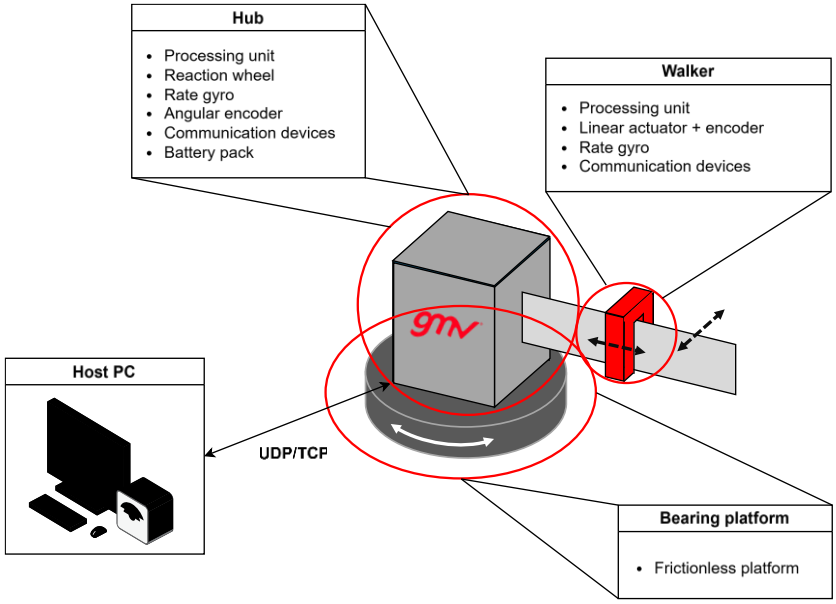

Fig. 2: Illustration of the concept for the platform, highlighting its main components.

Fig. 3 depicts the architecture of the system, with a particular focus on the selected avionics. Its main elements are:

- A central hub, mounted on top of a low friction platform. This central element hosts the main board (Raspberry Pi) where the GNC software is executed, the reaction wheel to control the attitude of the platform, the attitude sensors, and a battery to power electronics and the reaction wheel.
- The reaction wheel is controlled and managed by a dedicated Arduino board, and interfaces with the wheel motor via a motor driver.
- The robotic walker is controlled by its own Arduino board and is powered by a battery attached to it, with wireless communication to the hub.

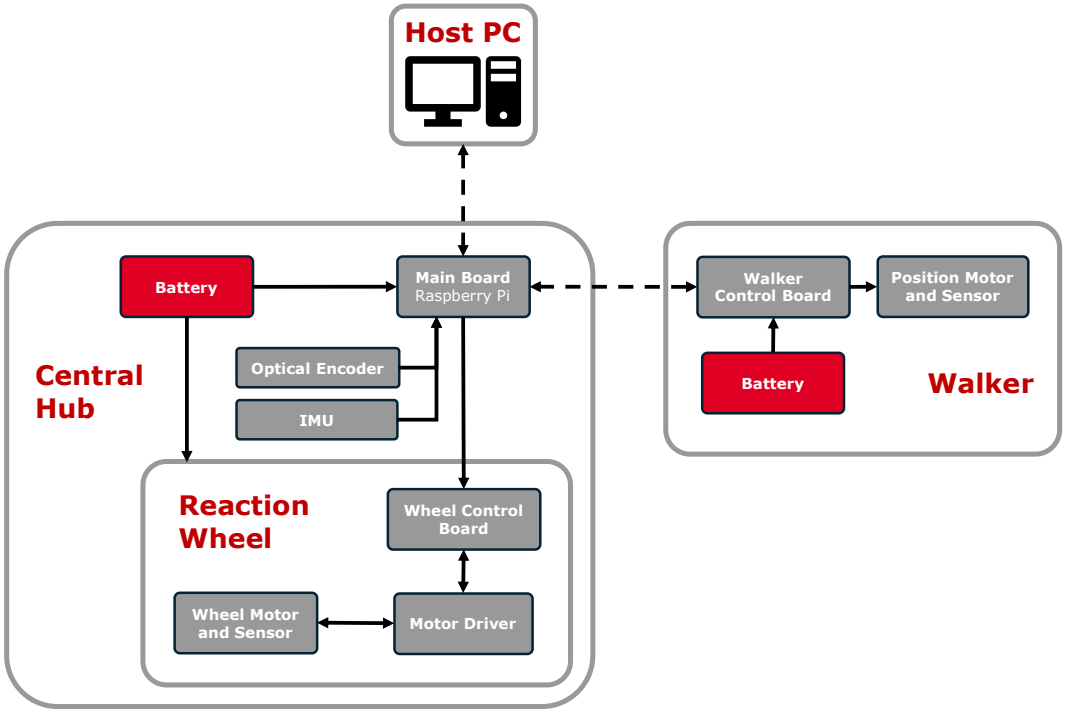

Fig. 3: Avionics and communications diagram.

The host PC handles software configuration, code generation, and telemetry data acquisition. Furthermore, it communicates wirelessly with the Main Board on the central hub which in turn communicates wirelessly with the walker control board, receiving IMU data and commanding translation profiles to the walker. This configuration, tied to the use of batteries, enables a setup with no cables and hanging elements which would otherwise impact the dynamics.

The software design is performed in MATLAB/Simulink for a rapid prototype development pipeline and fast development and verification iteration. The chosen hardware components have MATLAB libraries available to integrate their drivers directly into the auto-coding process, automatizing the deployment and HIL tests.

2.1 Low Friction Platform

The structure of the TRACTOR was designed as a testbed that is lightweight, low-friction, modular, and easy to calibrate to evaluate GNC solutions, composed of a static assembly and a rotating assembly. A schematic of the testbed is presented in Fig. 4.

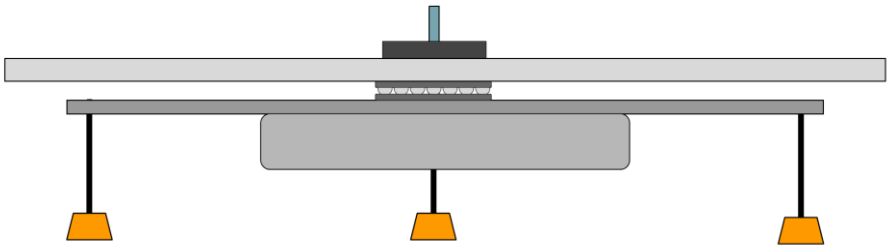

Fig. 4: Schematic of static and rotating assemblies in the TRACTOR-beam testbed.

The static assembly is the base of the structure that supports the rotating assembly, providing a flat reference surface for calibration and serving as the tracking surface for the optical encoder. A triangular steel base sits on three adjustable feet, forming a determinate (three-point) support that allows levelling

perpendicular to the local gravity vector. It also houses a thrust ball bearing for axial support and a shaft to bear lateral displacements.

The rotating assembly carries the actuators, electronics, batteries, sensors, beam, and robotic walker. The upper platform is a gridded plate that provides a modular mounting pattern for components.

2.2 Flexible Beam

Structural dynamics is not a topic commonly discussed in detail for GNC applications and is usually treated as just an input for control design. In TRACTOR, it is important to understand the underlying dynamics to select an adequate beam.

In a first approximation, the beam with the walker can be modelled as an Euler-Bernoulli beam with a discrete mass, a common approach for preliminary modelling of solar panels. However, such approximation is no longer applicable when the sliding mass is not at the tip. If the mass is located at an intermediate point, then the suspended beam mass after the sliding mass also affects the dynamics. The beam-mass system is better approximated as a two-segment beam with a mass, where the two segments are split right at the mass position.

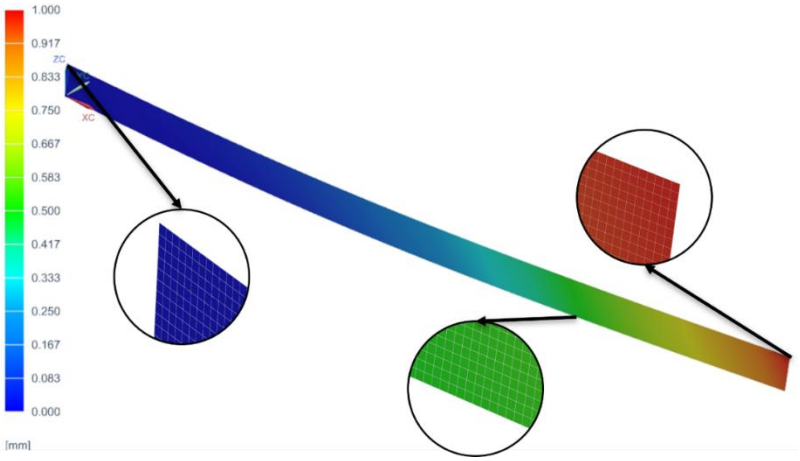

Fig. 5: FEA for an Aluminium beam: close-up views highlight the mesh and some normalized displacements.

The dynamic model for the platform-beam-walker system, described in more detail in Section 3.1, is based on a modal effective mass approach [12]. The outcome of the structural analysis is a matrix of modal participation factors ($\mathbf{L}_k$) and an associated natural frequency ω_{0k}. The estimation of the beam properties is obtained using two methods:

- Based on an analytical formulation of a two-segment beam with a discrete mass, where the corresponding mode shapes and natural frequencies are derived using continuous systems theory.
- Based on a Finite Element Analysis (FEA) like shown in Fig. 5, adding a discrete mass to the nodes where the robotic walker is located, and performing a numerical modal decomposition.

The results of both methods are then compared against experimental results as described in Section 4.1, showing a reasonable agreement between the experimental, FEA and analytical approaches. The experimental results are used to improve the parametrization of the analytical approaches and feed the dynamic model in Section 3.1.

2.3 Robotic Walker

The robotic walker is a motorized system that moves along the flexible beam. It was developed in-house to meet the requirements of the platform and experiments, and the benefits of the design are twofold:

- The position of the walker on the beam changes its mass distribution, which in turn changes the natural frequencies of the entire system. Higher natural frequencies are obtained when the walker is closer to the hub, decreasing when the walker moves towards the tip. This behaviour is analogous to a metronome.
- The total inertia of the system varies with the position of the walker, which in turn has an important impact on the overall attitude dynamics.

A diagram showing the components of the robotic walker is provided in Fig. 6, as well as a picture of the final version produced. For enhanced stability, the walker body wraps the beam. A set of wheels contact the beam sideways to produce traction, and these are driven by a small motor. This enables position control of the walker with enough accuracy to perform the experiments. All the avionics on the robotic walker are powered by a battery and connect wirelessly to the outside systems, eliminating the need for suspended wires.

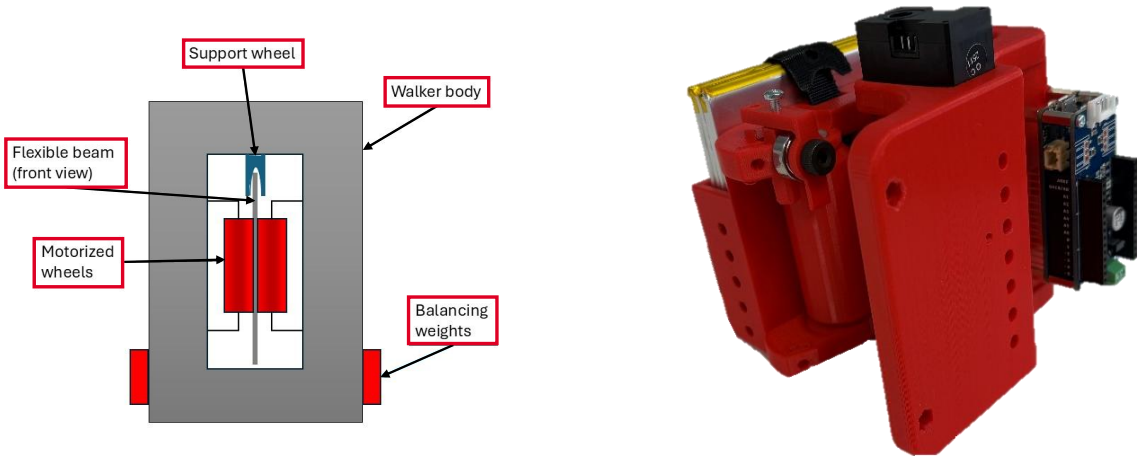

Fig. 6: Robotic walker diagram and final product.

There are support wheels on top of the robot to improve contact with the beam. The combination of support wheels and motorized wheels produces a statically determined system, minimizing slack to avoid additional vibrations.

The robot is balanced by design to have its centre of mass as close as possible to the central axis of the beam. This reduces any torsion introduced by an off-balance in the system. Additionally, there are slots on its body that can be used to mount balancing masses.

2.4 Actuators, Sensors and Navigation

Both the actuators and sensors have been selected and/or developed with quick MATLAB integration in mind and representativity for space applications.

The actuation and disturbances are introduced using a reaction wheel developed in-house as can be seen marked in Fig. 1. The reaction wheel was selected as the actuation mechanism to replicate the dynamics of in-orbit actuation systems: Effects like command and momentum saturation and

management, internal dynamics and micro-vibrations are critical considerations for control systems in space.

On the other hand, replicating typical attitude determination sensors for orbit applications is more difficult on-ground. Star trackers recognize star patterns to determine their own “absolute” attitude. Selecting sensors like absolute rotational encoders could become a problem if there is a misalignment in the system, because it could cause contacts and introduce friction. Using “relative” sensors such as gyroscopes was not an acceptable option either, since the accuracy of the angle estimation degrades over time. The final decision involved adapting an optical flow sensor to work as a rotational encoder. The sensor, along with a high-contrast surface to improve detection, have been included in the testbed, as shown in Fig. 7. This approach provides relatively accurate angular measurements with fast sampling times. The data can be processed, down sampled and fused with an IMU to reproduce the inputs of in-space gyro-stellar estimators.

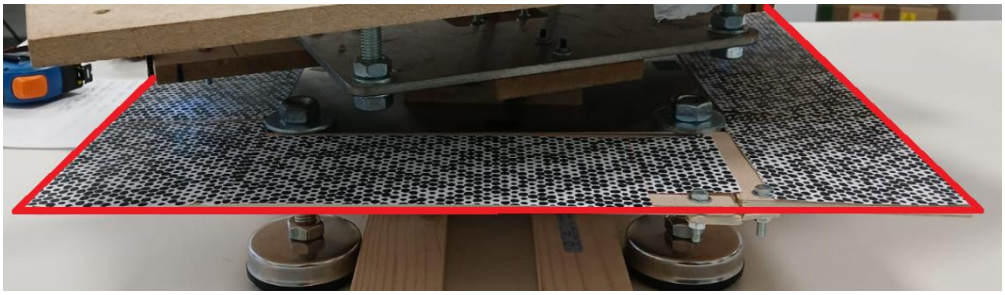

Fig. 7: Surface for optical flow detection on the TRACTOR-Beam platform.

Finally, the position of the robotic walker is estimated by in-motor contactless absolute encoders during translational control. The position accuracy has proven to be acceptable for the desired application, being transmitted to the hub for controller scheduling purposes and other relevant tasks based on the system properties. On top of that, there is an IMU embedded in the walker to record additional telemetry for further analysis and post-processing.

3 Digital Twin and Rapid Prototyping

3.1 System Dynamics and Modelling

The dynamic model is based on a combination of the platform dynamics presented in [2] with the modal participation and coupling model presented in [11]. Fig. 8 shows the different contributors to the platform dynamics, each of which is described in more detail later in this section.

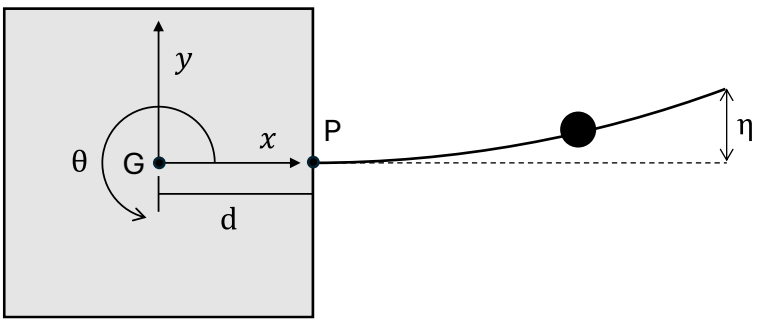

Fig. 8: Platform schematics, reference frame and relevant variables.

Fig. 9 shows the inverse coupled dynamic model of the central hub and the flexible beam.

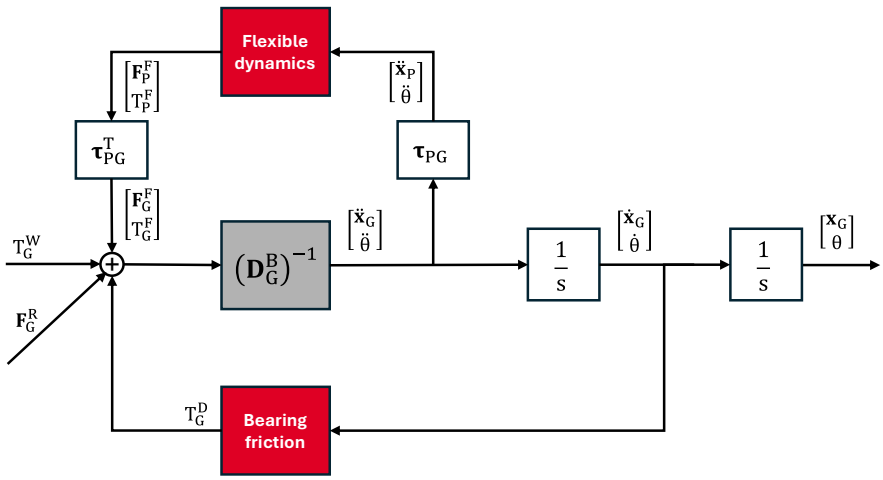

Fig. 9: Block representation of the dynamics of the platform.

The dynamics of the platform are given by

$$\begin{bmatrix} \ddot{x}_G \\ \ddot{\theta} \end{bmatrix} = \mathbf{D}_G^{B^{-1}} \left(\begin{bmatrix} 0 \\ T_G^W \end{bmatrix} + \begin{bmatrix} F_G^F \\ T_G^F \end{bmatrix} + \begin{bmatrix} 0 \\ T_G^D \end{bmatrix} + \begin{bmatrix} F_G^R \\ 0 \end{bmatrix} \right), \tag{1}$$

where the accelerations are expressed at the rotation point of the platform (G). Equation (1) accounts for the wheel torque (T_G^W), the flexible force F_G^F and torque T_G^F, the friction torque on the central platform (T_G^D), and the lateral force that keeps the central platform in place (F_G^R). $\left(\mathbf{D}_G^B\right)^{-1}$ represents the inverse mass and inertia matrix expressed at point G, the rotation axis of the platform.

The flexible dynamics expressed at the beam attachment point (P) are represented by the modal second order system in (**2**) and (**3**),

$$\begin{bmatrix} F_P^F \\ T_P^F \end{bmatrix} = [\mathbf{L}_P^T\mathbf{K} \quad \mathbf{L}_P^T\mathbf{D}] \begin{bmatrix} \boldsymbol{\eta} \\ \dot{\boldsymbol{\eta}} \end{bmatrix} + (\mathbf{L}_P^T\mathbf{L}_P - \mathbf{D}_P^A) \begin{bmatrix} \ddot{x}_P \\ \ddot{\theta} \end{bmatrix} \tag{2}$$

$$\begin{bmatrix} \dot{\boldsymbol{\eta}} \\ \ddot{\boldsymbol{\eta}} \end{bmatrix} = \begin{bmatrix} 0 & \mathbf{I} \\ -\mathbf{K} & -\mathbf{D} \end{bmatrix} \begin{bmatrix} \boldsymbol{\eta} \\ \dot{\boldsymbol{\eta}} \end{bmatrix} + \begin{bmatrix} 0 \\ -\mathbf{L}_P \end{bmatrix} \begin{bmatrix} \ddot{x}_P \\ \ddot{\theta} \end{bmatrix} \tag{3}$$

where $\mathbf{L}_P$ denotes the participation factor matrix, and $\mathbf{K}$ and $\mathbf{D}$ denote the stiffness and damping matrices, respectively. These parameters are obtained using the analysis described in Section 2.2. The excitation of each mode is represented by the modal coordinate η (see Fig. 8). The forces and torques need to be transformed between point P and G using the matrices $\boldsymbol{\tau}_{PG}$. Additionally, the platform friction is given by

$$T_G^D = \begin{bmatrix} 0 & 0 \\ 0 & -\sigma \end{bmatrix} \begin{bmatrix} \dot{x}_G \\ \dot{\theta} \end{bmatrix} \tag{4}$$

Finally, the lateral force in the rotation axis is such that the linear acceleration at centre of rotation G is 0. With all this developed, the system can be grouped as a single transfer function for controller purposes, as given by

$$\ddot{\theta} = M(s)T_G^W \tag{5}$$

The model presented is Linear Time Invariant (LTI) and can only represent the change of robotic walker position as “slices” of this LTI model. With this approach, the walker mass and its position is not explicitly modelled in the equations, but rather it appears implicitly in the definition of the beam participation factors. This is enough for control design and testing and approximates well the stability of the system. However, there are ongoing developments to include the time derivatives of the walker

position to ensure proper conservation of angular momentum and even non-linear terms. Additionally, the friction model used only considers a viscous term, while it would be more interesting to include more complex friction curves such as the dynamic model presented in [13].

3.2 Simulation Environment

To streamline development, a Simulink simulation environment was created to facilitate rapid synthesis and prototyping of GNC solutions before deployment on the real platform. Fig. 10 depicts the high-level diagram of the Simulink implementation.

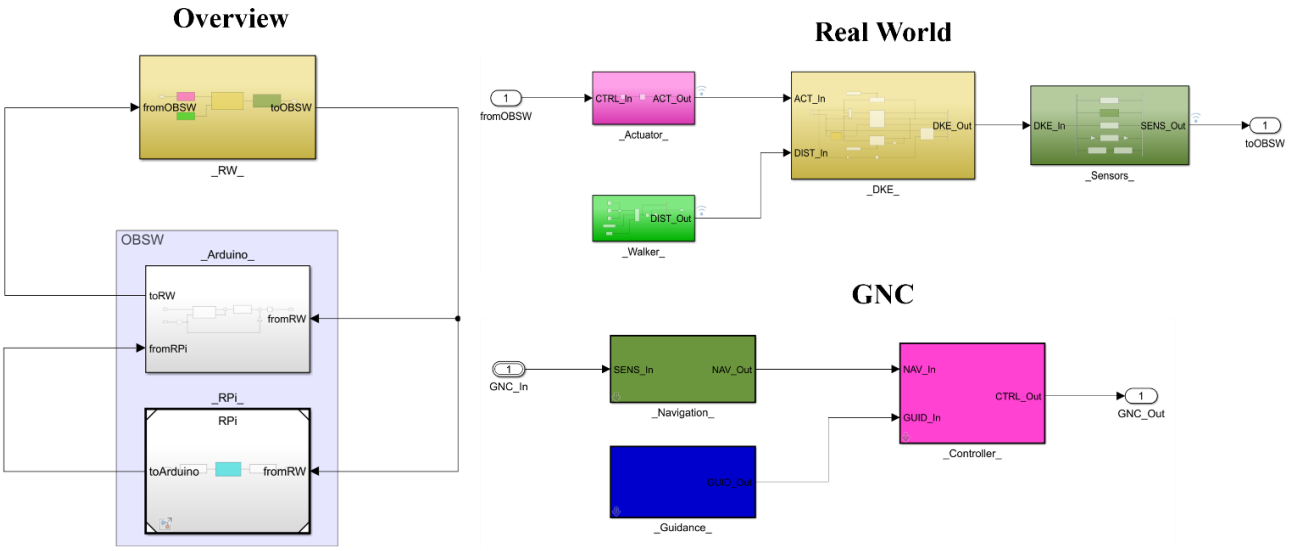

Fig. 10: Simulink environment.

To increase the representativity of the simulation environment, an attempt was made to include all the relevant inter-connections of the system, hardware limitations, sampling times, and operational caveats. In particular, the GNC modules (Navigation, Guidance, Controller) were designed and implemented inside a Simulink target subsystem, enabling auto-coding and execution on a Raspberry Pi 4B running on the central hub. On top of that, the GNC functions were implemented within Simulink libraries, and all the pre- and post-processing OBSW routines were added to the target subsystem. To complete the OBSW, the management and control of the reaction wheel - handled by an Arduino board - were emulated in Simulink.

In addition to the OBSW functions, the digital twin also includes representative analytical models for the different parts of the platform. In particular, the actuation subsystem, walker dynamics, hub dynamics, and sensors are modelled with the goal of simulating the real-world dynamics. In specific:

- The reaction wheel dynamics (_Actuator_ subsystem) are modelled with an integrator on the control torque scaled by the flywheel inertia, coupled to a viscous friction term whose coefficient was identified experimentally.
- The walker dynamics (_Walker_ subsystem) represent the open-loop translation profile commanded to the walker. Its internal dynamics and feedback loop are handled by the walker control board.
- The dynamics, kinematics, and environment of the hub (_DKE_ subsystem), described in Section 3.1, include both the rigid- and flexible-body dynamics of the hub, as well as the environment disturbances, in this case characterized by the platform bearing friction.
- The sensors (_Sensors_ subsystem) used by the GNC, which include

- an IMU unit for measuring the angular rate of the hub,
    - an IMU unit for measuring the angular rate of the walker,
    - an optical encoder for measuring the angular position of the hub,
    - a position sensor on the walker, and
    - a Hall effect encoder for measuring the speed of the reaction wheel.

This architecture offers a streamlined framework for MIL, SIL, and PIL testing of the GNC. SIL tests can be quickly conducted using MATLAB Embedded Coder and Simulink Coder toolboxes. Similarly, PIL tests can be seamlessly performed by connecting to the hardware and deploying the auto-coded functions onto the RPi via the target subsystem (*_RPI_* subsystem). The ultimate advantage of such approach is that the main GNC functions do not have to be manually coded into C/C++ language as this is automatically handled by MATLAB, also handling the cross-compilation. Finally, the GNC library is linked to a HIL model, which leverages Simulink support packages for RPi communication, allowing the replacement of the real-word block in Fig. 10 by the actuation, sensing, and remaining avionics interfaces of the main board. This enables rapid prototyping, experiment monitoring, and allows real-time telemetry visualization in Simulink.

3.3 DDVV and Auto-Coding Pipeline

TRACTOR-Beam fits in the pipeline of model-based design and prototyping, and provides a tool for more rapid development cycles. Preliminary design, detailed design, implementation and testing usually follow a linear pattern, with each stage feeding back into the others.

With a Simulink implementation, the availability of a digital twin, and appropriate licenses, new algorithms can be evaluated in simulation, uploaded and tested onto the platform in a matter of minutes. Fig. 11 illustrates the integration of Simulink within the platform, providing an interface for MIL, SIL, PIL, and HIL tests. The architecture presented in Section 3.2 highlights a clear separation between the dynamics and the OBSW functions. The latter can be transformed into C-code, compiled, uploaded to the testbed and executed using available tools in MATLAB.

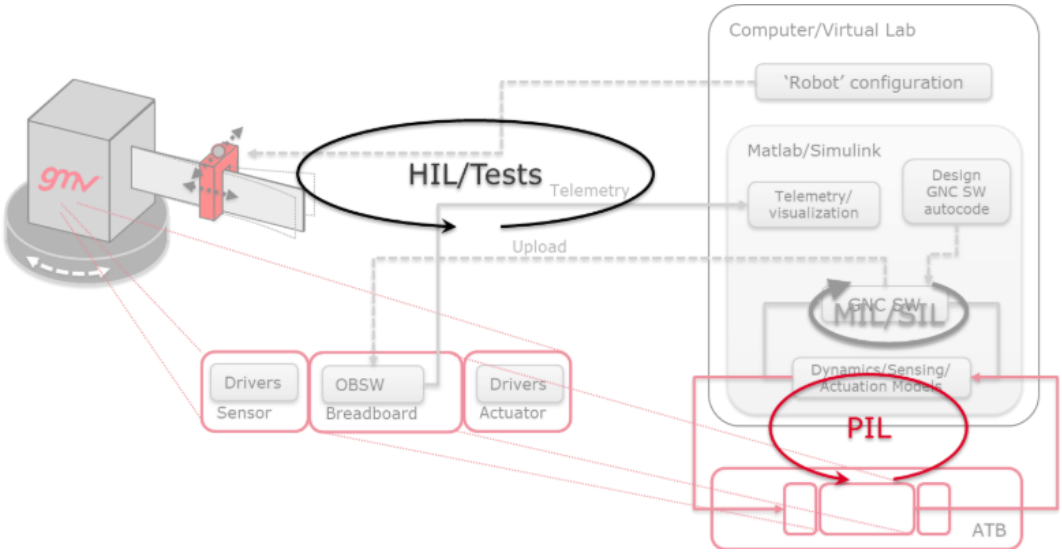

Fig. 11: SW architecture to support MIL, SIL, PIL, and HIL tests.

4 Preliminary Results

4.1 System Identification

An extensive System Identification campaign has been performed to characterize the system and obtain a reliable digital twin. The campaign includes multiple layers of characterization, with some approaches seeking to align a physical model to the experimental data in the time domain, others matching a pre-defined transfer function to frequency domain data, and others relying on full black-box estimates. All these are combined to obtain representative models for the different behaviours of the platform and overall dynamics.

Fig. 12 shows an analysis matching the natural frequencies of the beam observed experimentally against several analytical methods used to predict them. These are obtained assuming a beam with cantilever boundary conditions, disregarding any coupled dynamics with the rest of the platform. The curves include an *analytical model* integrating the equations of a flexible beam with an attached mass, and Finite Element Analysis (FEA) with two different tools, a FEM implementation in MATLAB and Siemens NX. These are compared against the measured experimental frequencies obtained through a Fourier analysis of the measured displacements, with all the results matching within 0.1 Hz of each other in the worst case.

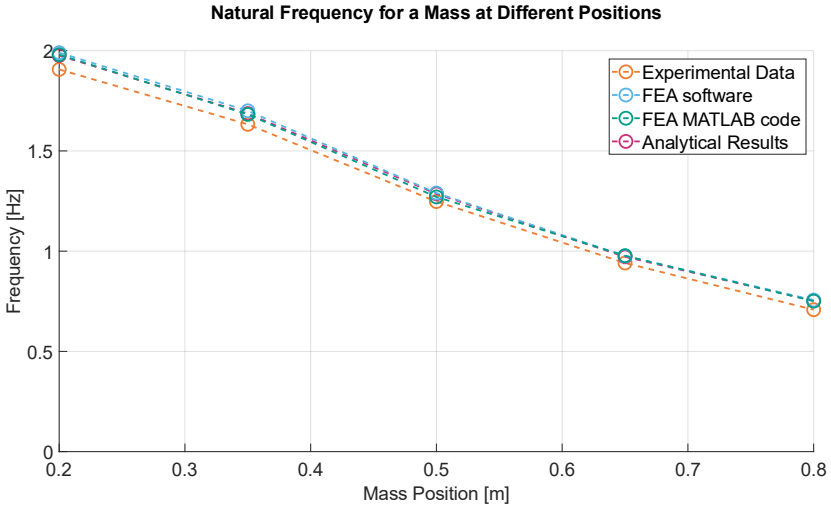

Fig. 12: Comparison of the beam's natural frequency obtained from analytical, FEA and experimental results.

The dynamics of the platform with the attached beam are a combination of dynamic effects driven by the beam's cantilever behaviour and additional contributing factors. Fig. 13 shows the Frequency-Response Data model (FRD) from MATLAB, including confidence intervals, obtained from a torque input based on a broadband-coloured noise signal, to the output measured angular rate. From the figure, there are two clear natural modes which come from two close pairs of poles and zeros. This result was obtained for a fixed walker position.

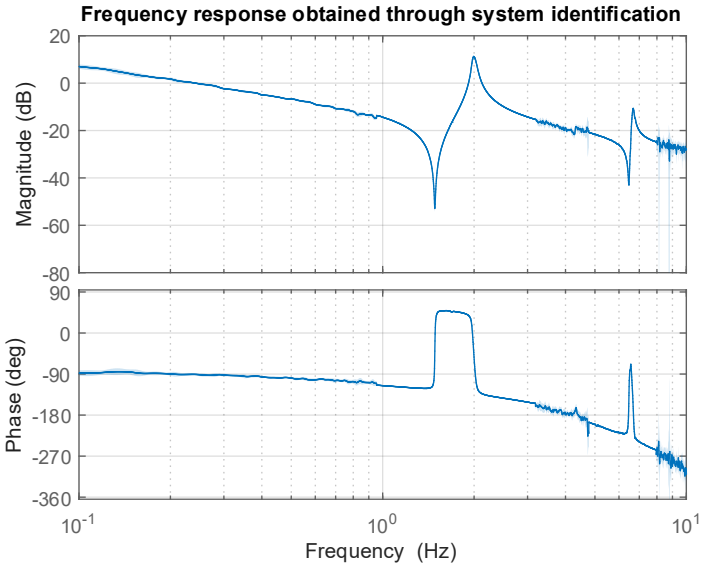

Fig. 13: FRD model for a fixed walker position subject to broadband coloured noise.

The results of a similar exercise for multiple sliding mass positions can be seen in Fig. 14, where a transfer function was fitted to the data considering the parametric model

$$\frac{\Omega(s)}{T(s)} = \frac{b_2 s^2 + b_1 s + b_0}{s^3 + a_2 s^2 + a_1 s} \tag{6}$$

with coefficients a_i and b_i identified using the `tfest()` function in MATLAB. For each position, the mass was fixed, and an entire sweep was performed generating the different curves. The figure shows one of the main goals of the platform: the natural frequency changes as the sliding mass moves, and the sliding mass produces a noticeable change in the inertia (which is observed by the change in low-frequency gain).

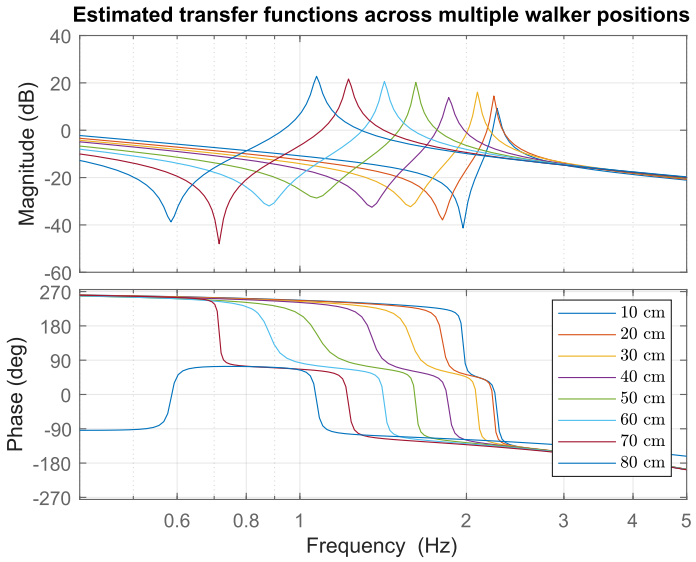

Fig. 14: Estimated transfer functions across multiple robotic walker positions.

Fig. 15 shows a manual matching of the physical parameters in the coupled platform-beam dynamic equations described in Section 3.1, to the analytical frequencies obtained in Fig. 12. The results demonstrate qualitative matching and a good level of agreement, although a more robust method for model alignment could be used. Nonetheless, this method enables the identification and alignment of

physical parameters with a time-varying, nonlinear model for the incorporation of a dynamic LPV model, on top of the current LTI model, which preserves angular momentum as the sliding mass moves.

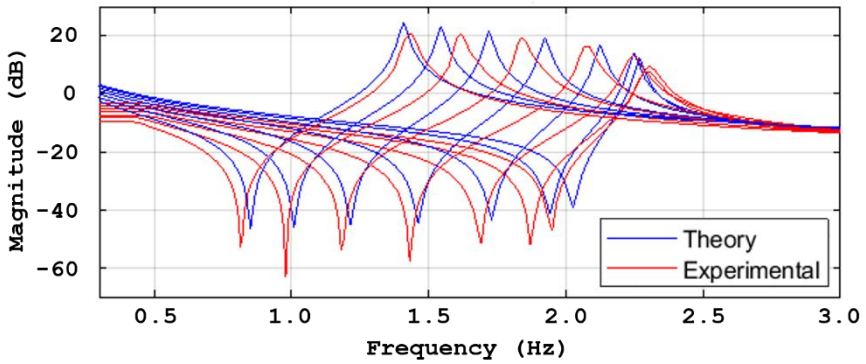

Fig. 15: Comparison between the model obtained via system identification and the analytical model derived from beam analysis.

These results demonstrate the suitability of the platform's actuation and sensing to explore and test system identification methods for systems with time-varying properties and bending modes, in a low friction setup to mimic ISAM.

4.2 Closed-loop MIL & HIL Results

The setup was used to test and compare simulated GNC in closed-loop against Hardware-in-the-Loop, performing all sensing, computation and actuation directly on the platform hardware. A simple GNC scheme was implemented to showcase the relevancy of the time-varying properties captured by the TRACTOR-beam platform. A static and adaptive Linear–Quadratic–Gaussian (LQG) controller was implemented, combining a Linear–Quadratic Regulator (LQR) for optimal state feedback and a Kalman filter for state estimation. To address the time-varying dynamics, a gain scheduling scheme was implemented, where the LQG gains were interpolated based on the position of the walker. This was done by computing the LQG gains for the eight identified models, corresponding to eight walker positions, and then linearly interpolating between them. The control law takes the form:

$$\begin{aligned} \dot{\hat{\mathbf{x}}} &= \mathbf{A}(\rho)\hat{\mathbf{x}} + \mathbf{B}(\rho)u + \mathbf{L}(\rho)(y - \mathbf{C}(\rho)\hat{\mathbf{x}}) \\ u &= -\mathbf{K}(\rho)\hat{\mathbf{x}} \end{aligned} \tag{7}$$

where ρ denotes the position of the robotic walker. To make the different controllers comparable, they all used the same weighting matrices.

Fig. 16 shows the step response for a 10-degree command while the walker moves along the beam and the controller gains are constant throughout the whole experiment. This test showcases the closed-loop capabilities of the platform and the need for adaptive controllers: It can command and maintain an attitude successfully within the constraints imposed by hardware, but it becomes unstable as the walker moves far from the initial position. The figure shows, from left to right, top to bottom: central hub angular position, control action, central hub angular rate and the walker position. Although the dynamics are comparable between real world and digital twin as shown in the previous section, there are effects that are not modelled to the full extent in this iteration of the MIL, such as detailed sensor modelling, which results in some of the noises and chatter differences.

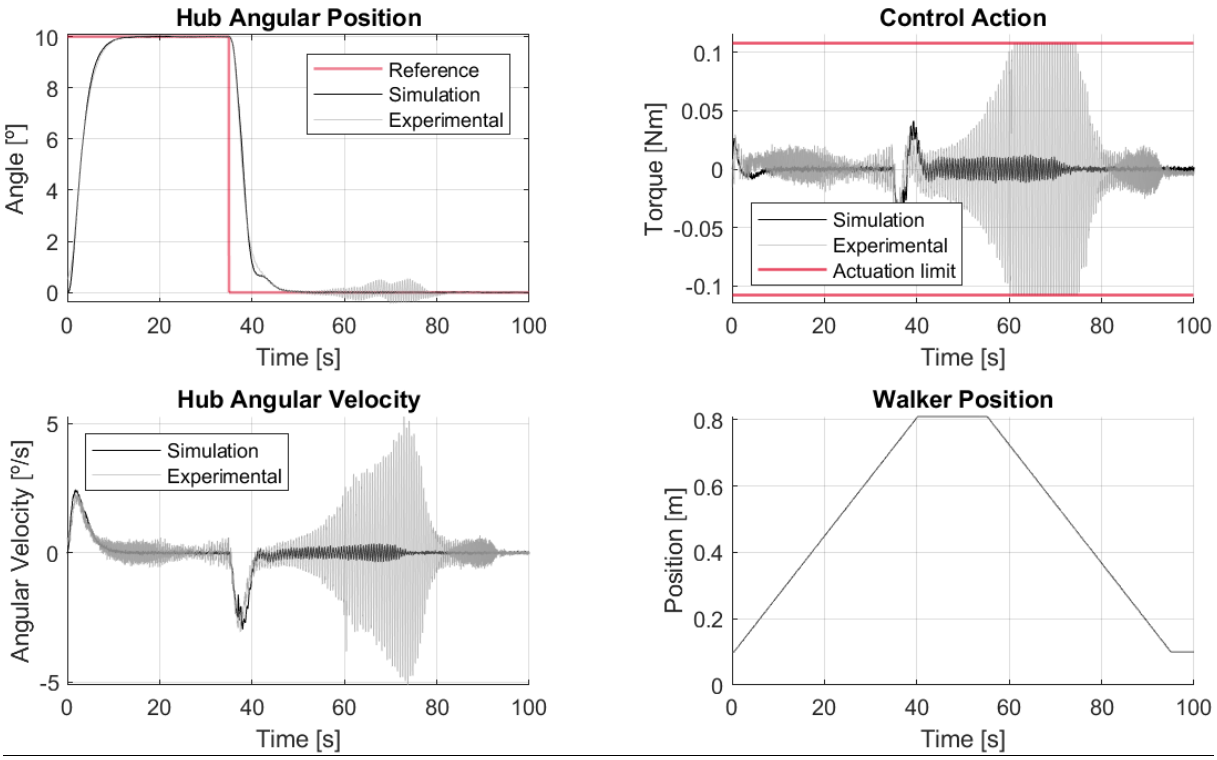

Fig. 16: Closed-loop experiment with walker motion and a non-scheduled controller.

Fig. 17 shows the results for a similar experiment as Fig. 16 but this time the controller gains are scheduled according to the system properties, using the robotic walker position as scheduling parameter. In this case, the system remains stable even when the properties change. These experiments show the time-varying capabilities of TRACTOR, its ability to excite complex and non-trivial dynamics, and the need for adaptive controllers.

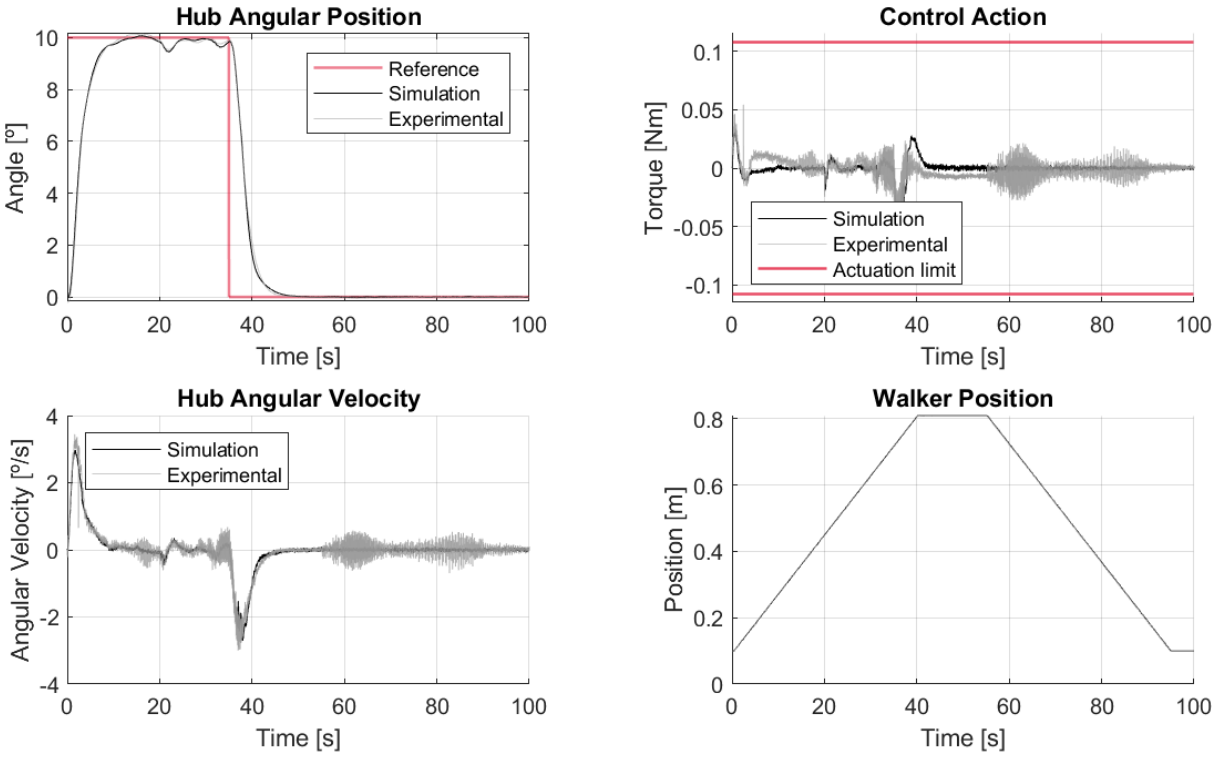

Fig. 17: Closed-loop experiment with walker motion and a scheduled controller.

5 Conclusions

This work introduces TRACTOR-Beam, a rotating platform with low-friction support and a wireless (cable-free) setup to minimize interference with the desired free motion dynamics. The platform includes a reaction wheel, a flexible beam, and a robotic walker that moves along the beam, actively changing the dynamics and natural frequencies of the system throughout the experiments. It provides a scalable and modular platform with space-representative sensors and actuators that aims to replicate the challenges of ISAM, while increasing the Technology Readiness Level (TRL) of GNC solutions.

The experimental platform features a modular architecture allowing quick reconfiguration (e.g., beam swapping, sloshing effects), and the range of dynamics successfully captures the challenges faced by GNC for systems with time-varying properties. The platform integrates a digital twin with MATLAB/Simulink, enabling the seamless transition from simulation to real-world testing, control design, and auto-coding. This architecture supports MIL, SIL, PIL, and HIL tests with fast deployment of on-board software.

The capabilities of the TRACTOR-beam platform have been successfully demonstrated. System identification using analytical models, FEA, and experimental data demonstrate variation of natural frequencies and control performance with the position of the walker. The presented results demonstrate how system identification can be used to generate dynamic models for simulation and control tuning. A representative GNC setup illustrates how the properties of the system have enough variation to impact the controller's stability and performance, justifying the need for adaptive and time-varying approaches. The GNC example suggested that the use of an adaptive controller, scheduled according to the position communicated by the walker, resulted in a clear robustness gain through the use of a time-varying control architecture.

We show how TRACTOR-Beam replicates the challenges of ISAM, bridging the gap between simulation and real-world testing for time-varying systems, and how it enables rapid prototyping and algorithm validation in a realistic, low-friction environment. It can be used for system identification, tuning of advanced control strategies, including gain scheduling and adaptive control, and validation of several GNC algorithms. Furthermore, it can improve ISAM mission readiness by providing a testbed for spacecraft with flexible and evolving dynamics.

Acknowledgments

We want to use this section to acknowledge Arkadiusz Groth, Emma Forgues-Mayet, Pedro Cachim and Luís Bessa Ferreira for their contributions to the first phases of the IOANT project that led to the development of this test platform. To Ionut Dragos Porcescu for his contributions to control validation, and for his help in setting up the initial versions of the digital twin. To Evangelos Papadopoulos, Georgios Rekleitis, and Kostas Nanos from the National Technical University of Athens for their help and comments during the development of the actuation system of the platform. To INEGI - Instituto de Ciência e Inovação em Engenharia Mecânica e Engenharia Industrial, and in particular to Ricardo Rocha for their support in the mechanical design and fabrication of the components.

The work of Eduardo de Brito on the development of avionics, estimation, system identification, and control of the platform was supported by Prof. Pedro Batista from IST. The work of Mariana Ferreira on the mechanical analysis, finite element and analytical modelling, and experimental characterization of the flexible elements of the platform was supported by Prof. Aurélio Araújo, also from IST.

The work presented in this report was carried out under, and funded by, the ARTES 4.0 Core Competitiveness Generic Programme Line (ESA Contract No. 4000138572/22/NL/AF “Guidance, Navigation And Control Of In-Orbit Assembly Of Large Antennas”). The views expressed herein can in no way be taken to reflect the official opinion of the European Space Agency.

Declaration of Use of Artificial Intelligence

Artificial intelligence was not used in the work presented.

References

[1] J. Briz et al. Guidance, navigation, and control of in-orbit assembly of large antennas – Technologies and approach for IOANT. In *Proceedings of the 41st ESA Antenna Workshop on Large Deployable Antennas*, Noordwijk, The Netherlands, September 2023. doi: 10.5281/zenodo.17227916.

[2] D. Alazard and R. Bouttes. BAMOSS: An experimental testbed for flexible structure dynamics modeling and control. In *Proceedings of the 2009 European Control Conference (ECC)*, August 2009, pp. 1167–1172. doi: 10.23919/ECC.2009.7074563.

[3] C. Nieto-Peroy, M. Sabatini, G. Palmerini, and É. Jeronimo de Oliveira. A concurrent testing facility approach to validate small satellite combined operations. *Aerospace*, 8(12), 2021. doi: 10.3390/aerospace8120361.

[4] Z. Huang, W. Zhang, T. Chen, H. Wen, and D. Jin. Characterizing an air-bearing testbed for simulating spacecraft dynamics and control. *Aerospace*, 9, 2022. doi: 10.3390/aerospace9050246.

[5] E. Papadopoulos, I. Paraskevas, G. Rekleitis, and F. Thaleia. The NTUA space robotics emulator: Design and experiments. In *Proceedings of the IEEE/RSJ International Conference on Intelligent Robots and Systems (IROS '11): Workshop on Space Robotics Simulation*, 2011.

[6] P. Colmenarejo, E. di Sotto, and J. A. Béjar. Dynamic test facilities as ultimate ground validation step for space robotics and GNC systems. In *Proceedings of the 6th International Conference on Astrodynamics Tools and Techniques (ICATT)*, 2016.

[7] L. Pasqualetto Cassinis, A. Menicucci, E. Gill, I. Ahrns, and M. Sanchez-Gestido. On-ground validation of a CNN-based monocular pose estimation system for uncooperative spacecraft: Bridging domain shift in rendezvous scenarios. *Acta Astronautica*, 196, 2022, pp. 123–138. doi: 10.1016/j.actaastro.2022.04.002.

[8] A. A. Ali, B. Beigomi, and Z. H. Zhu. Development of 6DOF hardware-in-the-loop ground testbed for autonomous robotic space debris removal. *Aerospace*, 11(11), 2024. doi: 10.3390/aerospace11110877.

[9] H. Benninghoff, F. Rems, E.-A. Risse, and C. Meitner. EPOS 2.0 RvD simulator. *Journal of Large-Scale Research Facilities*, 3, 2017. doi: 10.17815/jlsrf-3-155.

[10] J.-C. Piedboeuf, J. de Carufel, F. Aghili, and E. Dupuis. Task verification facility for the Canadian special purpose dextrous manipulator. In *Proceedings of the 1999 IEEE International Conference on Robotics and Automation*, Detroit, MI, USA, 1999, pp. 1077–1083. doi: 10.1109/ROBOT.1999.772461.

[11] D. Alazard, C. Cumer, and K. Tantawi. Linear dynamic modeling of spacecraft with various flexible appendages and on-board angular momentums. In *Proceedings of the 7th International ESA Conference on Guidance, Navigation & Control Systems (GNC 2008)*, Tralee, Ireland, June 2008, pp. 1–14.

[12] A. Girard and N. Roy. *Structural dynamics in industry*. Wiley & Sons, 2008.

[13] B. Armstrong and C. C. de Wit. Friction modeling and compensation. In *The Control Handbook*. CRC Press, 1995.